

## Dynamic Compression of an Interpenetrating Phase Composite (IPC) Foam: Measurements and Finite Element Modeling

Chandru Periasamy and Hareesh Tippur  
Department of Mechanical Engineering  
Auburn University, AL 36849  
[htippur@eng.auburn.edu](mailto:htippur@eng.auburn.edu)

### ABSTRACT

Dynamic compression response of Syntactic Foam (SF)–aluminum foam Interpenetrating Phase Composites (IPC) is measured. By infusing uncured syntactic foam (epoxy filled with hollow microballoons) into an open-cell aluminum network, a 3D interpenetrating structure is obtained. The uniaxial compression responses are measured at ~1500 /sec using a split Hopkinson pressure bar set up. The effect of volume fraction of microballoons on the compression response of IPC is examined in terms of yield stress, plateau stress and energy absorption. The response of IPC samples are also compared with those made using syntactic foam alone. For all volume fractions of microballoons, the IPC samples have better compression characteristics when compared to the corresponding syntactic foam samples. The failure modes of SF and IPC foams are examined both optically (using high-speed photography) and microscopically. The measured dynamic responses of SF are used in a finite element model based on a Kelvin cell representation of the IPC structure. Using infinite elements and measured particle velocity histories as input boundary conditions, the compression response of IPC foams have been successfully captured.

### INTRODUCTION

Aerospace, automotive and marine industries demand novel multifunctional material solutions for structural problems. A class of composites called Interpenetrating Phase Composites (IPC) [1] has been gaining reputation recently mainly for their multifunctional capabilities. The IPC used in this work is a syntactic foam (SF) - aluminum foam based IPC. Syntactic foam is made by mixing hollow glass microballoons in epoxy. The IPC is made by infusing uncured syntactic foam into open cell aluminum foam prior to curing. In the current work, high-strain rate (~1500 per second) compression properties of IPCs made of four different volume fractions ( $V_f$ ) of microballoons in SF are analyzed and compared with the pure SF counterparts. Surface analysis of real time deformation of samples and microscopic analysis of sectioned samples are also performed to understand the failure mechanisms. A unit cell based finite element model of the IPC is developed in which the aluminum structure is idealized as a tetrakaidecahedron (a 14 sided polyhedron) called Kelvin cell [2]. Experimentally measured material properties of SF are used for the SF region in the computational model. Infinite elements [3] are used to model the far field region surrounding the unit cell. Finite element results of IPC compare well with those from experiments.

### MATERIAL SPECIFICATIONS

The SF foam is prepared by first mixing low viscosity epoxy (Epo-Thin™ from Beuhler, Inc. USA, mass density of resin ~1100 kg/m<sup>3</sup>) and hollow glass microballoons (K-1™ microballoons from 3M Corp., bulk density 125 kg/m<sup>3</sup>) of average diameter ~60 μm and wall thickness ~0.6. The uncured SF is then transferred into a silicone rubber mold after vacuuming to remove any trapped air bubbles. The mixture is then allowed to cure for seven days before being removed and machined to size. The aluminum foam used in the IPC is a commercially available open-cell Duocel® aluminum (Al6101-T6) foam (ERG aerospace Corp., with a pore density of 40 pores per inch; ~8% relative density). The metal foam is cleaned with acetone and then coated with silane to enhance the bond strength between the aluminum ligaments and the SF. To prepare the IPC, the degassed, uncured SF is prepared the same way as before. Then, the silane coated aluminum foam is slowly inserted into the mold containing the uncured syntactic foam so that the syntactic foam fills in the open pores of the aluminum network. After curing, the unfinished sample is removed from the mold for machining. The length and diameter of the machined samples used in the dynamic tests are 9.5 mm and 12.7 mm, respectively.

## EXPERIMENTAL RESULTS

SF and IPC samples with 10%, 20%, 30% and 40% microballoon volume fractions in SF were tested at a strain rate of  $\sim 1500$  per second using a split Hopkinson pressure bar (SHPB) [4] developed for this purpose. The stress-strain responses, energy absorption capacities and failure processes of SF and IPC samples are discussed below.

### Stress-strain response

The dynamic true stress – true strain response of syntactic foam has two distinct regions (Fig 1(a)). An initial linear elastic response is followed by a monotonically decreasing stress region with increasing strain. The compressive strengths of the 10%, 20%, 30% and 40% volume fraction SF samples are approximately 104 MPa, 80 MPa, 62 MPa and 50 MPa, respectively. The relative decrease in the compressive strengths for every 10% increase in the microballoon volume fraction is  $\sim 20\%$ . The tendency for the SF with lower volume fraction of microballoons (10% and 20%) to soften after attaining the maximum stress is somewhat more distinct than for the ones with higher volume fraction of microballoons (30% and 40%). After yielding, the stresses for SF with lower  $V_f$  of microballoons remain consistently higher than that for SF with higher  $V_f$ . The difference in stress values after yielding between specimens with different volume fraction of microballoons is approximately constant at all strains (within the observation window). The dynamic compression response (Fig 1(b)) of IPC foams follow trends similar to that of the corresponding  $V_f$  syntactic foams. In the order of increasing microballoon  $V_f$ , the maximum stress values attained by IPC are approximately 120 MPa, 100 MPa, 80 MPa and 60 MPa. The percentage decrease in the compressive strength for the IPC-20 with respect to that of IPC-10 is 17%, and that of IPC-30 with respect to that of IPC-20 is 20%. The IPC-40 has a 25% decrease in compressive strength with respect to the IPC-30. In general, for all volume fractions, the yield strengths of IPC are higher than that of corresponding SF.

### Energy absorption

The energy absorbed per unit volume by SF and IPC were evaluated up to a strain value of 22% as  $U_{0.22}$  and are shown in Fig 2. Energy absorbed by SF-10, SF-20, SF-30 and SF-40 samples are 21.9 MJ/m<sup>3</sup>, 19.6 MJ/m<sup>3</sup>, 16.4 MJ/m<sup>3</sup> and 12.1 MJ/m<sup>3</sup>, respectively and that by IPC-10, IPC-20, IPC-30 and IPC-40 samples are 24.5 MJ/m<sup>3</sup>, 22.0 MJ/m<sup>3</sup>, 18.3 MJ/m<sup>3</sup> and 12.7 MJ/m<sup>3</sup>, respectively. The percentage reduction in  $U_{0.22}$  per unit volume for the SF-20 / SF-10, SF-30 / SF-20 and the SF-40 / SF-30 pairs are approximately 11%, 16% and 26% respectively. The percentage reduction in  $U_{0.22}$  per unit volume for the IPC-20 / IPC-10, IPC-30 / IPC-20 and the IPC-40 / IPC-30 pairs are approximately 10%, 17% and 30%, respectively. The trend of the percentage reduction in the energy absorption per unit volume suggests that the rate of reduction in  $U_{0.22}$  would be greater than the rate of increase of the microballoon volume fraction for dynamic loading. Also, IPC samples have higher energy absorption capacities per unit volume when compared to corresponding SF samples.

### Failure progression

Another interesting outcome under dynamic loading conditions is strain recovery in SF and IPC foam samples. The final lengths of the deformed samples were measured after the tests for both SF and IPC. Interestingly, for SF samples, the final measured lengths were more than that predicted by the SHPB equations following a 25% engineering strain. This suggests that the SF samples had partially recovered (sprung-back) after deformation.

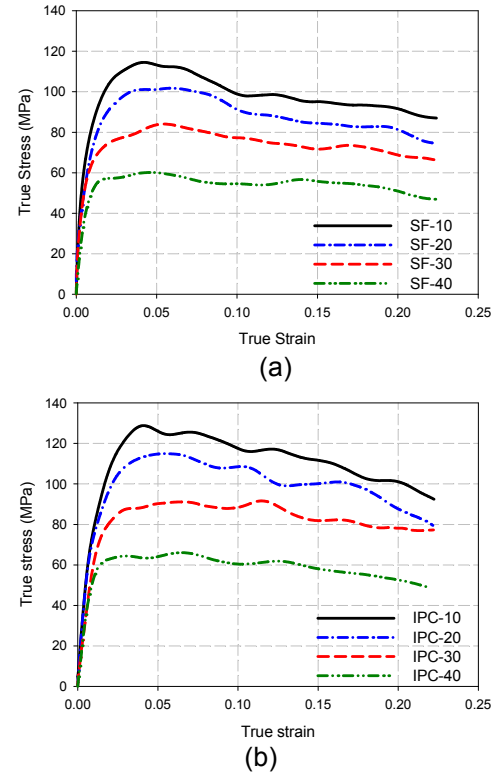


Figure 1: Dynamic compression responses of (a) SF and (b) IPC foams (Strain rate  $\sim 1500/s$ )

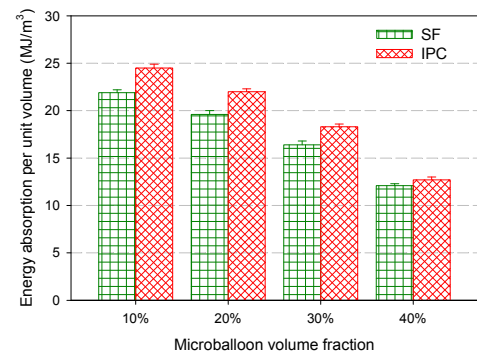


Figure 2: Energy absorbed per unit volume by SF and IPC under dynamic loading up to 22% true strain

However, this phenomenon was negligible in case of IPC samples. The spring back in the SF is potentially overcome in the IPC by the aluminum ligaments. Once aluminum ligaments undergo plastic deformation, they prevent the SF from spring-back. The spring-back phenomenon was verified by recording the failure of SF and IPC foams in real-time using high-speed photography. Backlit photographs of deformed SF and IPC samples with 30%  $V_f$  of microballoons are shown in Fig 3. A network of shear bands crisscrossing the entire sample and oriented at approximately  $\pm 45^\circ$  to the loading direction can be readily seen. Micrographs of deformed 30%  $V_f$  SF and IPC specimens are shown in Fig 4. The cracks that appear in the images are skewed at an angle of approximately  $45^\circ$  to the direction of application of the load suggesting failure due to shear localization. In regions away from the crack, the microballoon footprints are circular suggesting very little deformation. However, shear bands in IPC are interrupted by the metallic ligaments. The other type of failure in IPC, which is absent in pure SF samples, is the debonding of the interfaces between the syntactic foam and the aluminum ligaments.

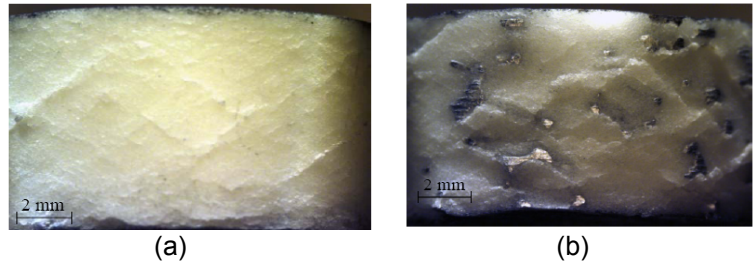


Figure 3: Side view of dynamically deformed (a) SF and (b) IPC samples (Loading was along the vertical direction)

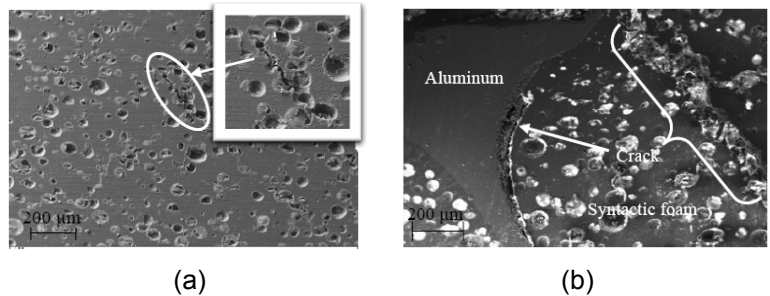


Figure 4: SEM image of cross section of dynamically deformed (a) SF and (b) IPC samples (Loading was along the vertical direction)

### FINITE ELEMENT MODELING

A unit cell finite element model of the IPC foam was used to predict the dynamic compression response. The geometry was modeled using the solid modeling software Solid Edge and imported into the finite element analysis software ABAQUS. The three dimensional connectivity of aluminum ligaments of the cell was modeled as an idealized 14 sided polyhedron (tetrakaidecahedron). Based on the measurements on the ligaments of the actual aluminum foam and the volume fraction of aluminum in the actual IPC, the dimensions of the ligament were chosen. Accordingly, the length of the ligaments is 1.5 mm and the cross section is triangular with  $\sim 0.78$  mm edges. In a dynamically loaded sample, stress waves travel through the entire length of the sample before reflecting at the end of the sample, whereas in the model the stress waves would get reflected at the boundaries of the cell itself.

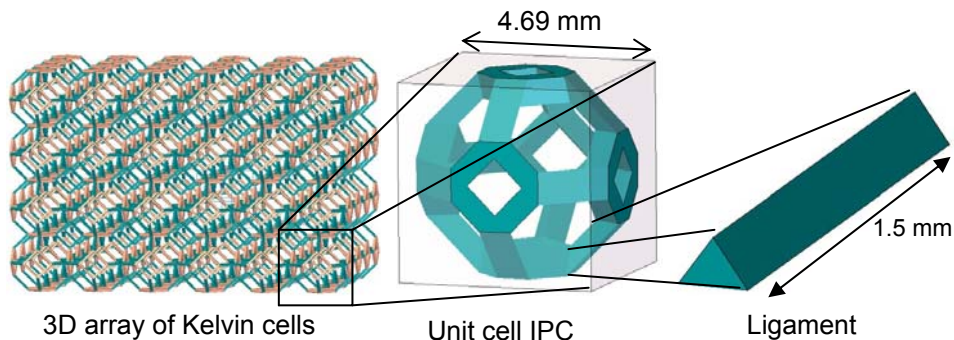


Figure 5: Schematics representing the building blocks of an idealized Kelvin cell based IPC

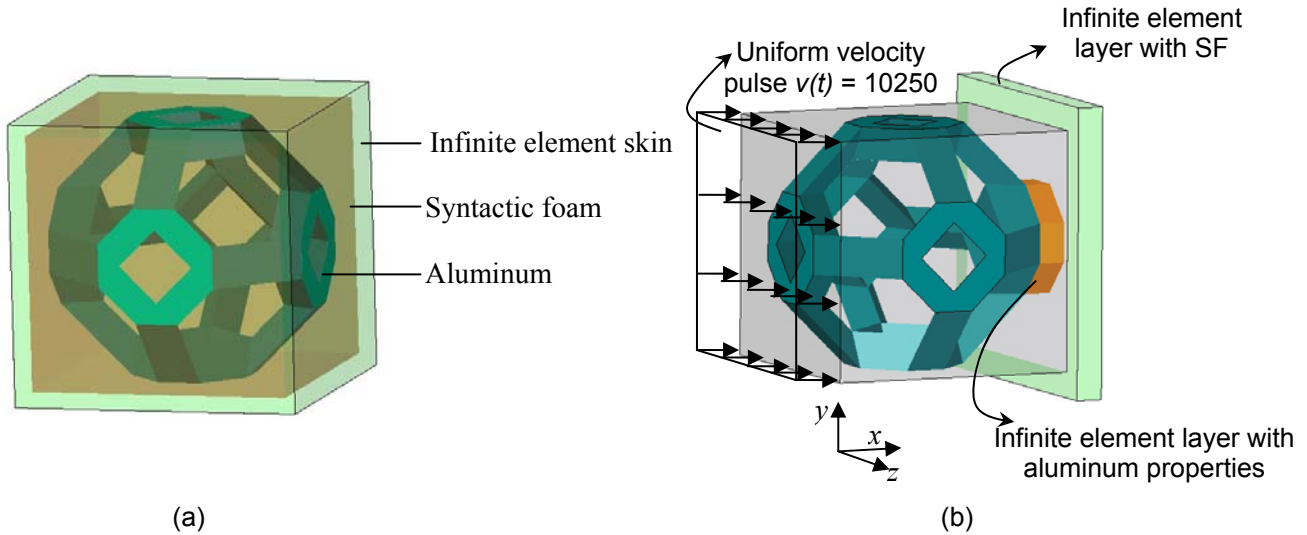


Figure 6: (a) Unit cell model with outer infinite element layer. (b) Load and boundary conditions

To overcome this shortcoming, a skin of SF and aluminum material was modeled adjacent to the corresponding material at the boundary of the cell. This skin was discretized using the so-called *infinite elements* to represent the far field regions surrounding the unit cell. Figure 5 shows the schematic of the building blocks of the model and the boundary conditions applied are shown in Figs. 6 (a) and (b).

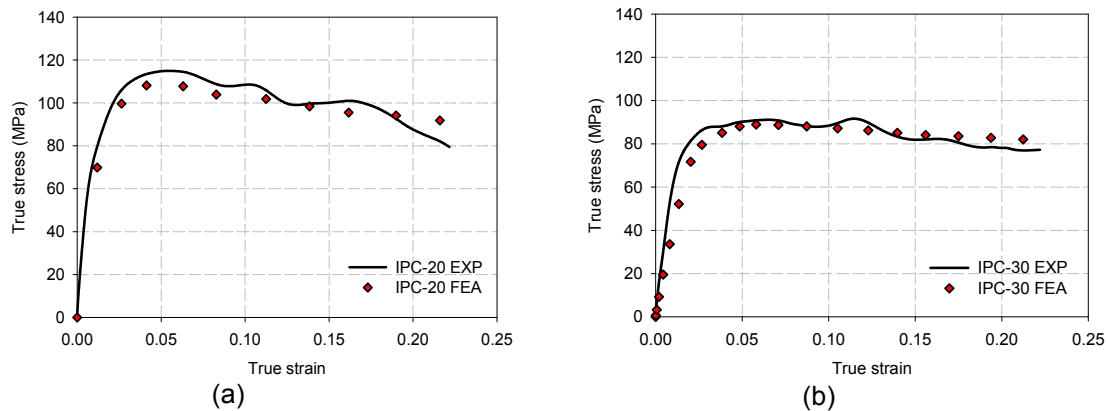


Figure 7: Comparison of experimental and FEA results of (a) IPC-20, (b) IPC-30

The measured particle velocity history (10250 mm/s for  $\sim 250$  microseconds) in the incident bar of the SHPB was used as the load input to the computational model. The input velocity pulse was applied on the surface of the unit cell which marks the boundary between the unit cell IPC and the infinite element layer on one side. IPC models corresponding to all four volume fractions of microballoons were simulated and the results are compared to that of the experiments. In Fig 7 the results for 20% and 30% volume fraction microballoons in SF are shown. Evidently, a good agreement between computations and measurements exists.

## SUMMARY

Uniaxial compression characteristics of Interpenetrating Phase Composite (IPC) foams have been studied under dynamic loading conditions using a split Hopkinson pressure bar apparatus. The IPC foams were made by infusing uncured epoxy-based syntactic foam (SF) into open-cell aluminum preforms. Curing of SF resulted in an IPC structural foam with a 3D interconnectivity. The dynamic compression responses of IPC foams made of SF with 10% - 40%  $V_f$  of hollow glass microballoons have been studied. The responses of IPC foams have also been evaluated relative to their pure SF counterparts. The  $V_f$  of microballoons in SF plays a dominant role in the overall

response of the SF and IPC foams studied. A monotonic increase in elastic modulus, yield stress, and plateau stress are evident as  $V_f$  of microballoons decrease. The IPC foams consistently have higher value of each of these characteristics relative to the corresponding SF. The energy absorbed per unit volume by the IPC under dynamic conditions is about ~10% higher than the SF counterparts. The failure of SF and IPC under dynamic conditions is dominated by the formation of an extensive network of shear bands in SF. In addition to microballoon crushing as seen in SF, IPC samples show debonding of aluminum ligaments from the surrounding SF. A unit cell model of the IPC using a space-filling polyhedron – tetrakaidecahedron has been successfully developed using ABAQUS. Infinite elements were used to model the far field region of the computational model. The stress-strain responses of the model IPC's have been compared to those from experiments. A good agreement between the simulated and the experimental results has been observed.

## REFERENCES

1. Clark D. R., 'Interpenetrating phase composites', *Journal of the American Ceramic Society*, 75(4), pp 739-759, 1992.
2. Thompson W (Lord Kelvin), 'On the division of space with minimum partitional area', *Philosophical Mag.*, 24, pp 503-514, 1887.
3. Bettess P, 'Infinite elements', *International Journal for numerical methods in engineering*, 11, pp 53-64, 1977.
4. Kolsky, H., 'An investigation of the mechanical properties of materials at very high rates of strain', *Proceedings of the Physical Society, Section B*, 62, 676-700, 1949.